JOURNAL OF AIRCRAFT
Vol. 38, No. 4, July–August 2001

Inverse Design of Transonic Wings Using Wing Planform and Target Pressure Optimization

Taisul Ahn*
Seoul National University, Seoul 151-742, Republic of Korea
Hyoung-Jin Kim†
Korea Aerospace Research Institute, Taejun 305-600, Republic of Korea
and
Chongam Kim‡ and Oh-Hyun Rho§
Seoul National University, Seoul 151-742, Republic of Korea

A new method is presented for an efficient inverse design of transonic wings with minimum drag and weight. To this end, the target pressure optimization method is extended for a simultaneous design of wing planform and target pressures so that an inverse design can be conducted with the optimized planform and section target pressures. During the optimization procedure, the maximum thickness of wing sections and spanwise lift distribution should be predicted without any flow analysis, and response surfaces are, therefore, constructed for this purpose. Sample data points for the response surfaces are selected from the *D*-optimality and calculated by a thin-layer Navier–Stokes code. For the optimization problem, a genetic algorithm is adopted. Design examples show that the present design method gives successful results with the computational cost reduced by one order of magnitude compared to a direct response surface construction for lift and drag coefficients.

Nomenclature

AR, TR	=	aspect ratio, taper ratio
C, S	=	wing section chord length, wing area
t/c	=	maximum thickness to chord ratio at a wing section
Λ, θ	=	sweep angle, twist angle

Subscripts

a	=	after inverse design
b	=	before inverse design
$ds0$, $ds1$, $ds2$	=	value at root, kink, and near-tip design section
0, 1, 2	=	value at the root, kink, and tip
00	=	value of baseline wing

Introduction

WITH the advances in computational fluid dynamics (CFD) and computing power of modern computers, aerodynamic design methods utilizing CFD codes are more important than ever before. Design methods applicable to aerodynamic design problems can be categorized into two classes: inverse design methods and direct optimization methods. The inverse design method determines the shape of an airfoil or a wing that produces a prescribed pressure distribution on its contour at a specified flow condition, whereas a direct optimization method tries to design an aerodynamic configuration by minimizing a given objective function, which is usually a function of aerodynamic coefficients such as C_L, C_D, or C_M. The inverse design method requires about 10–20 flow analyses[1,2] and can be expected to be more efficient than a direct optimization method, which may need more than 100 flow analyses[3] unless an adjoint method[4] is not adopted for the sensitivity analysis.

Received 14 May 1999; revision received 31 May 2000; accepted for publication 16 February 2001.

*Graduate Research Assistant, Department of Aerospace Engineering.
†Senior Researcher, Aero-Propulsion Research Department. Member AIAA.
‡Assistant Professor, Department of Aerospace Engineering. Member AIAA.
§Professor, Department of Aerospace Engineering. Senior Member AIAA.

However, the inverse design methods have a few drawbacks compared to the direct optimization methods. First, inverse design methods require aerodynamic designers to specify a target pressure distribution producing improved aerodynamic performance and satisfying structural and manufactural constraints. Although experienced aerodynamicists can identify desirable flow characteristics, for example, reduced shock strength and/or elimination of flow separation, it is not a trivial task to develop a target pressure distribution that will provide these benefits while maintaining other aerodynamic requirements such as lift and pitching moment. To overcome this defect, several researchers investigated numerical optimization of the target pressure for an inverse design of subsonic/transonic airfoils[1,2,5,6] and wings.[2] Van Egmond[5] developed a target pressure optimization method and applied it to transonic and subsonic airfoil design cases. Aerodynamic shape functions were defined for a parameterization of the pressure distribution. He pointed out that the target pressure optimization problem is strongly nonlinear and exhibits discontinuous derivatives for the objective as well as constraint functions. This severe nonlinearity motivated the use of genetic algorithms (GAs) instead of gradient-based optimization algorithms in the target pressure optimization problems. Obayashi and Takanashi[6] applied a GA to the target pressure optimization for transonic and subsonic wing section designs. They used the *B*-spline interpolation for the parameterization of the target pressure. Kim and Rho[1,2] also applied a GA to the target optimization for the transonic airfoils[1] and wings.[2] They considered three-dimensional features, such as spanwise wing loading distribution and a shock wave or isobar line sweep angle for a successful design of transonic wings.

The second drawback of the inverse design method is the lack of versatility in a sense that it is difficult for the inverse method to be extended to more general design problems, such as multipoint design, wing planform design, multidisciplinary design optimization (MDO), etc. The direct optimization methods, on the other hand, are very versatile, that is, they can be extended to other design problems and combined with other design tools with relative ease.

Because of the limitation of the inverse method, little research has been conducted in MDO problems with the inverse method. Recently, however, Takahashi et al.[7] designed a transonic wing with a sequential multidisciplinary approach including an inverse design method. First, they optimized wing planform shape with minimum

drag and wing weight and maximum fuel weight. Second, target pressure distribution was optimized for the predesigned wing planform using a GA and then an inverse design was conducted to produce the final wing section geometry. However, they did not have control of the maximum thickness of wing sections in the first design stage. A proper maximum-thickness prediction method for the inverse design was not suggested.

The main purpose of the present study is to apply the inverse design method to a multidisciplinary design problem of transonic wing planform and section shape design. To this end, the target pressure optimization code using a GA developed in Ref. 2 is extended to a simultaneous design of wing planform and target pressure optimization (WTO). In the WTO process, no CFD analysis is conducted, and therefore, every performance parameter needed should be calculated or estimated through prediction models developed a priori. For example, it was necessary to build an accurate prediction model for the maximum thickness of wing sections because the wing section thickness is a prerequisite for the wing weight and wave drag estimation. Another required model is a spanwise lift distribution prediction model because the spanwise wing loading also needs to be known without any CFD analysis during the optimization. The two prediction models mentioned earlier are developed by the response surface method (RSM). With the optimized wing planform and target pressures at design sections, an inverse design is conducted to determine final wing section geometry.

Following this introduction, a brief review on the flow analysis will be presented. Some details of the genetic optimization of the wing planform and target pressures will then be given including response surface model construction. Design examples and conclusions follow.

Flow Analysis

A three-dimensional Navier–Stokes solver developed and validated in Refs. 2 and 8 is used for the flow analysis. Three-dimensional Reynolds-averaged thin-layer Navier–Stokes equations in generalized coordinates are used in the conservation form based on a cell-centered finite volume method. Roe's flux difference splitting scheme with the MUSCL (see Ref. 9) approach is adopted for the spatial discretization. Jameson and Yoon's[10] lower–upper symmetric Gauss–Seidel method is used in the implicit part. Turbulence effects are considered using the Baldwin–Lomax model with a relaxation technique. We used a C–O grid system around a wing with 135 points in the streamwise direction, 41 points in the normal direction, and 30 points in the spanwise direction. Although somewhat coarse grids are used, it is shown in Ref. 2 that this grid system captures accurate surface pressure distributions and gives aerodynamic coefficients comparable with the result of fine grids.

To build up a baseline wing, the root section of a wing designed by Kim and Rho[2] is used in the root section and the RAE2822 airfoil is adopted in outboard sections. The design conditions for all of the design cases in this study are $M_\infty = 0.78$ and $Re = 1.0 \times 10^7$ based on the root chord length. Density residuals are reduced by four orders of magnitude starting the calculation from a freestream value.

Inverse Design Method

We used a three-dimensional inverse design code,[2] which adopts the following Modified-Garabedian Mcfadden (MGM) equation (see Ref. 11) to solve an inverse problem at chordwise wing sections:

$$F_0 \Delta z + F_1 \Delta z_x + F_2 \Delta z_{xx} = R, \qquad (R = Cp_t - Cp_c) \quad (1)$$

where R is the residual, which is the difference between the target and computed pressure, and coefficients F_0, F_1, and F_2 are nonnegative constants chosen to provide a stable iterative process. In this study, the coefficients of the derivative terms are determined by local flow conditions on the wing surface. If the local flow is subsonic, the coefficient F_1 of the first derivative term is set to zero. Otherwise, the coefficient F_2 of the second derivative term is set to zero. In either case, only two out of three terms remain on the left-hand side. Then the MGM method becomes similar to the direct iterative curvature method.[12] The switching Mach number between the subsonic and supersonic flow was set to $1.1/\sin\Lambda_{1/2}$ by applying the simple sweep theory. The MGM equation (1) is then solved using a finite difference scheme.

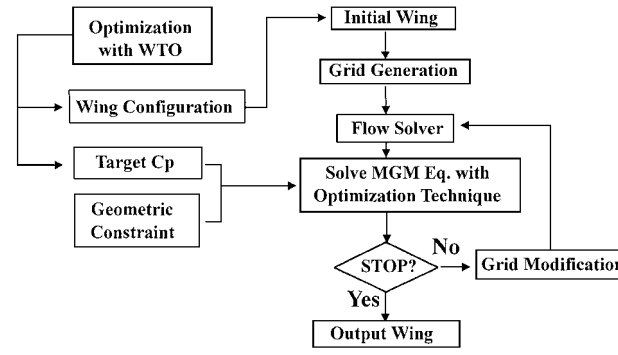

Fig. 1 Flowchart of the inverse design method.

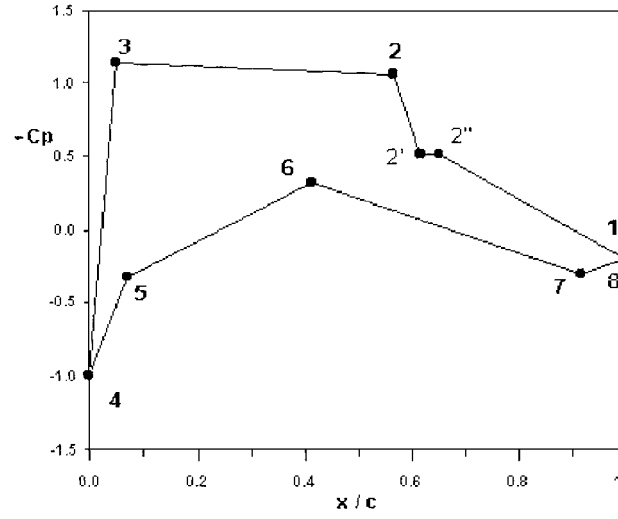

Fig. 2 Schematic representation of a target pressure distribution.

Figure 1 shows a flowchart of the inverse design procedure. A grid system is generated around a wing with the given planform and wing section shapes. Pressure distributions are computed by the flow analysis, and vertical displacements of the design section shapes are obtained by the inverse design method, and smoothed. The new design section shapes are then fitted to a 10th-order polynomial. Wing sections other than the design sections are interpolated from the design sections by the C-spline interpolation method inboard and by the linear interpolation outboard. Then the grid system is modified algebraically for the new wing geometry. This inverse design cycle is repeated until the geometric modification is sufficiently small. In practice, 12 design cycles are enough to obtain the final wing geometry.

WTO

Design Variables

Instead of using wing section shape parameters directly, those for target pressure distributions are adopted as design variables for the wing section design. Figure 2 shows a characteristic surface pressure distribution for a typical transonic wing section defined by eight points. Aerodynamic shape functions are used for interpolation between these points. The locations of characteristic points, local Mach numbers of the characteristic points, and the coefficients of shape functions are used as design variables. The number of design variables is 15 for a design section. Because 3 design sections are used in this study, the total number of design variables for the target pressure distributions is 45.

The target pressure can be generated at each design section of a wing in a two-dimensional manner. However, three-dimensional

Table 1 Ranges of design variable

Indices	Design variable	−1 (Lower bound)	0 (Center)	1 (Upper bound)
1	Λ, deg	25	29	34
2	θ_0, deg	4	5	6
3	θ_2, deg	0	1	2
4	C_0	0.8	1.0	1.2
5	TR_1	0.4	0.55	0.7
6	TR_2	0.2	0.3	0.4
7	y_2	1.9	2.4	2.9
8	y_1/y_2	0.291	0.333	0.375
9	$(t/c)_{ds0}$[a]	0.13	0.14	0.15
10	$(t/c)_{ds1}$[a]	0.085	0.100	0.115
11	$(t/c)_{ds2}$[a]	0.085	0.100	0.115

[a]For response surface modeling only.

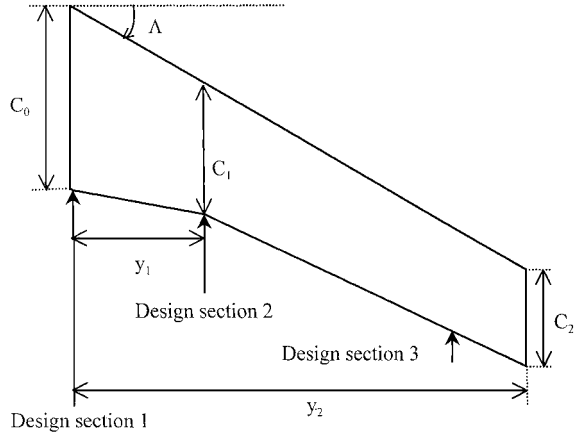

Fig. 3 Wing planform design variables.

characteristics, such as spanwise wing loading distribution and shock sweep angles or isobar-line sweep angles, are considered in the target pressure optimization procedure. Readers are referred to Ref. 2 for further details of the target pressure optimization method.

Design variables defined for wing planform are shown in Fig. 3. An incidence angle at the kink section, θ_1, is linearly interpolated from the root and tip angles based on the spanwise location. Three design sections are defined as the root, kink section, and a near-tip section located at 87.5% of outboard $\{y_1 + 0.875 \times (y_2 - y_1)\}$. Table 1 shows design variable ranges allowed in this study. All of the length scales are normalized by the root chord length of $DC - 9/30$ (Ref. 13).

Among the 11 design parameters listed in Table 1, the maximum thickness distributions at three design sections $[(t/c)_{ds0}, (t/c)_{ds1}$, and $(t/c)_{ds2}]$ are just employed for the response surface construction of themselves and not used in the WTO process. This is because the maximum thickness of a design section is not an independent design parameter, but a function of the integration of target pressures and other wing planform parameters as will be shown later.

Therefore, the total number of design variables for the WTO is 53, that is 45 for the target pressures at three design sections and 8 for the wing planform and twist angles.

RSM

The RSM[14–16] has been widely used to obtain a relationship between a specified response and a number of independent variables. The relationship is usually modeled by a second-order polynomial, which can be written for n variables as follows:

$$y = \lambda_0 + \sum_{i}^{n} \lambda_i x_i + \sum_{i}^{n} \sum_{i}^{n} \lambda_{ij} x_i x_j + \varepsilon \tag{2}$$

where x_i are design variables, λ_i are regression coefficients, y is the measured response, and ε represents the total error. The second-order model of Eq. (2) has $p = (n+1)(n+2)/2$ regression coefficients. For k sample data points, Eq. (2) can be written in a matrix form as

$$\{y\} = [X]\{\lambda\} + \{\varepsilon\} \tag{3}$$

where vector $\{y\}$ has k dimensions and the matrix $[X]$ is a $[k \times p]$ matrix. We can determine the vector of regression coefficients $\{\lambda\}$ using the method of least squares so that L_2 norm of the error vector $\{\varepsilon\}$,

$$L \equiv \sum_{i=1}^{k} \varepsilon_i^2$$

is minimized:

$$\{\lambda\} = ([X]^T \cdot [X])^{-1} \cdot [X]^T \cdot \{y\} \tag{4}$$

It can be shown that one can improve the fitting quality by minimizing $([X]^T[X])^{-1}$. It is shown in Ref. 17 that minimizing $([X]^T[X])^{-1}$ can be replaced by maximizing the determinant of $([X]^T[X])$. A method that uses a data point set $[X]$ maximizing the determinant of $([X]^T[X])$ is referred to as D-optimal design.[17] D-optimal point selection requires at least p sample data points, and it is known that 1.5–2 times of p is enough to get reasonable results.[16]

Prediction of Wing Section Thickness

In the inverse design of transonic wings, one of the main concerns for the specification of target pressure distributions is the prediction of the maximum thickness of a design section that has the prescribed target pressure distribution. To deal with this problem, van Egmond[5] suggested the following relation for the airfoil maximum thickness:

$$\left(\frac{t}{c}\right) \cong -\frac{\sqrt{1 - M_\infty^2}}{2} \int c_p \, \mathrm{d}x \tag{5}$$

Although this relation is not well tuned and may give inaccurate estimations, it was found that wing sections with the same spanwise position and the same value of the right-hand side of Eq. (5) have almost the same thickness ratio for a fixed twist angle and wing planform.[1,2]

However, if the wing planform and twist angles are also varied during the design process, a more robust prediction method is required for an accurate prediction of the maximum thickness before the wing section geometry is obtained through an inverse design. In this study, we defined the following relation between the integration of wing section surface pressures and design variables.

$$\int c_p \, \mathrm{d}x = -\frac{a_1 (t/c) + a_2}{\sqrt{1 - (M_\infty \cos \Lambda)^2}} + f \tag{6}$$

where f is a quadratic polynomial as Eq. (2) and a_1 and a_2 are additional regression coefficients.

The regression coefficients in Eq. (6) are functions of 11 design variables: 8 wingplanform variables and 3 maximum-thickness-to-chord ratios of three design sections $\{(t/c)_{d0}, (t/c)_{d1}, (t/c)_{d2}\}$. This requires more than 100 data points to be calculated for the response surface construction. To reduce the computational burden, we conducted an analysis of variation (ANOVA) to screen out design variables with little effect on the response. From this, we obtained the following reduced relations:

$$\int (c_p)_{ds0} \, \mathrm{d}x = -\frac{a_{01} (t/c)_{ds0} + a_{02}}{\sqrt{1 - (M_\infty \cos \Lambda)^2}} + f\left[\Lambda, \theta_0, \theta_2, C_0, \mathrm{TR}_1, y_1, \left(\frac{t}{c}\right)_{ds0}, \left(\frac{t}{c}\right)_{ds1}\right] \tag{7}$$

$$\int (c_p)_{ds1}\,\mathrm{d}x = -\frac{a_{11}(t/c)_{ds1} + a_{12}}{\sqrt{1-(M_\infty \cos\Lambda)^2}} + f\left[\Lambda, \theta_0, \theta_2, C_0, \mathrm{TR}_1, y_1, \left(\frac{t}{c}\right)_{ds1}\right] \tag{8}$$

$$\int (c_p)_{ds2}\,\mathrm{d}x = -\frac{a_{21}(t/c)_{ds2} + a_{22}}{\sqrt{1-(M_\infty \cos\Lambda)^2}} + f\left[\Lambda, \theta_0, \theta_2, C_0, \mathrm{TR}_1, \mathrm{TR}_2, \left(\frac{t}{c}\right)_{ds1}, \left(\frac{t}{c}\right)_{ds2}\right] \tag{9}$$

Because the maximum number of design variables in the preceding reduced models is 8 at the first and third design sections, the maximum number of regression coefficients for the preceding three response surface models is $47(=(8+1)(8+2)/2+2)$. We selected 65 sample data points from the D-optimal condition and performed Navier–Stokes computations accordingly.

When the regression coefficients are determined by the RSM, each of Eq. (7–9) becomes a quadratic equation for the maximum thickness-to-chordratio (t/c). It was found that the smaller root of the two solutions of the quadratic equation was always the right answer having a reasonable value whereas the larger solution is much greater than the smaller one by an order of magnitude.

The thickness prediction models were evaluated by calculating R^2, adjusted R^2 (adj-R^2), and the percent root mean square error (%rmse) for the data points used to construct the models.[14,15] The statistical terms are defined as follows:

$$R^2 \equiv 1 - (SS_E/S_{yy}) \tag{10}$$

where

$$SS_E = \sum_{i=1}^{n}(y_i - \hat{y}_i)^2 \qquad S_{yy} = \sum_{i=1}^{n} y_i^2 - \left[\left(\sum_{i=1}^{n} y_i\right)^2 \Big/ n\right]$$

$$\text{adj-}R^2 \equiv 1 - \frac{SS_E/(n-p)}{S_{yy}/(n-1)} = 1 - \left(\frac{n-p}{n-1}\right)(1-R^2) \tag{11}$$

$$\%\text{rmse} \equiv 100\sqrt{\frac{1}{n}\sum_{i=1}^{n}(y_i - \hat{y}_i)^2} \Big/ \frac{1}{n}\sum_{i=1}^{n} y_i \tag{12}$$

where n is the number of data points, p the number of regression coefficient, y_i a measured response for each data point, and $\hat{y}_i$ a predicted response for each data point. The response surface models can be considered to be reliable if the adj-R^2 value is greater than 0.9. Table 2 shows that the thickness prediction models have a reliable prediction capability.

Prediction of Spanwise Lift Distribution

To predict spanwise lift distributions of candidate wings without any flow analysis during the optimization process, a response surface model for the lift prediction should be built. In the present study, a lift prediction model is built by using both of the RSM and Weissinger's method (see Ref. 18), which is a modified lifting line theory for swept wings. The discrepancy between a spanwise lift distribution obtained by the Navier–Stokes solver and one by Weissinger's method is approximated by a 10th-order polynomial.

$$(cc_l)_{\mathrm{CFD}} = (cc_l)_{\mathrm{Weiss.}} + \Delta cc_l, \qquad \text{where} \qquad \Delta cc_l = \sum_{n=0}^{10} b_n \eta^n \tag{13}$$

where the coefficients b_n of the 10th-order polynomial are obtained by the quadratic response surface model of Eq. (2). Although there are 11 design variables listed in Table 1 for the response model construction, an ANOVA revealed that only five design variables, such as $\Lambda, \theta_0, \theta_2$ TR_1, and TR_2, can be employed with little accuracy degradation.

For the 5 design parameters, 35 data points are randomly selected among the 65 data points used for the thickness prediction models. Even when more than 35 data points were selected, the prediction accuracy was almost the same. Lift distributions at a sample data point is shown in Fig. 4, where it can be noted that the lift distributions obtained by the CFD and the lift prediction model compare well with each other. The %rmse for all of the data points (65 sample points) is 1.94% when a prediction error at a data point is defined as follows:

$$\text{error} = \frac{\sqrt{\sum\{(cc_l)_{\mathrm{CFD}} - (cc_l)_{\mathrm{predicted}}\}^2}}{\sum (cc_l)^2_{\mathrm{CFD}}} \tag{14}$$

We also tried a 10th-order polynomial model that does not employ Weissinger's method as follows:

$$(cc_l)_{\mathrm{CFD}} = \sum_{n=0}^{10} b_n \eta^n \tag{15}$$

Table 2 Accuracy of maximum thickness prediction models

Thickness-to-chord ratio	R^2	adj-R^2	%rmse
$(t/c)_{ds0}$	0.9722	0.9011	1.12
$(t/c)_{ds1}$	0.9707	0.9306	2.41
$(t/c)_{ds2}$	0.9926	0.9737	1.21

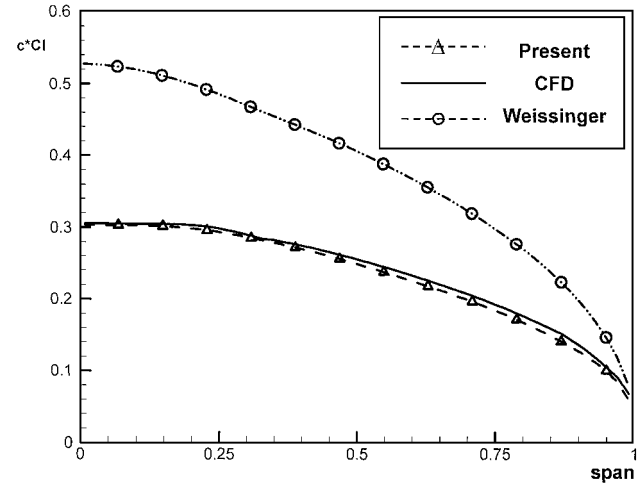

Fig. 4 Results of the lift distribution prediction at a sample data point.

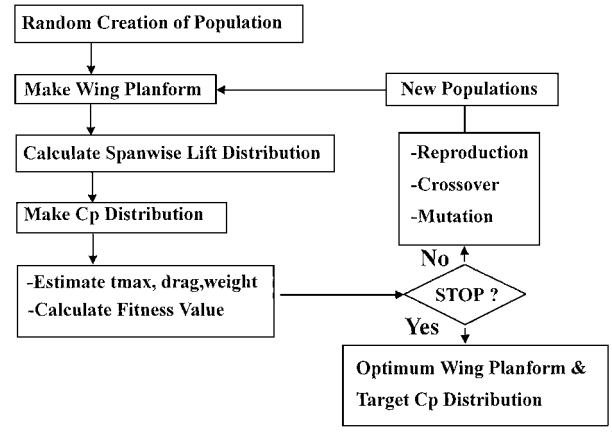

Fig. 5 Flowchart of the genetic optimization of wing planform and target pressures.

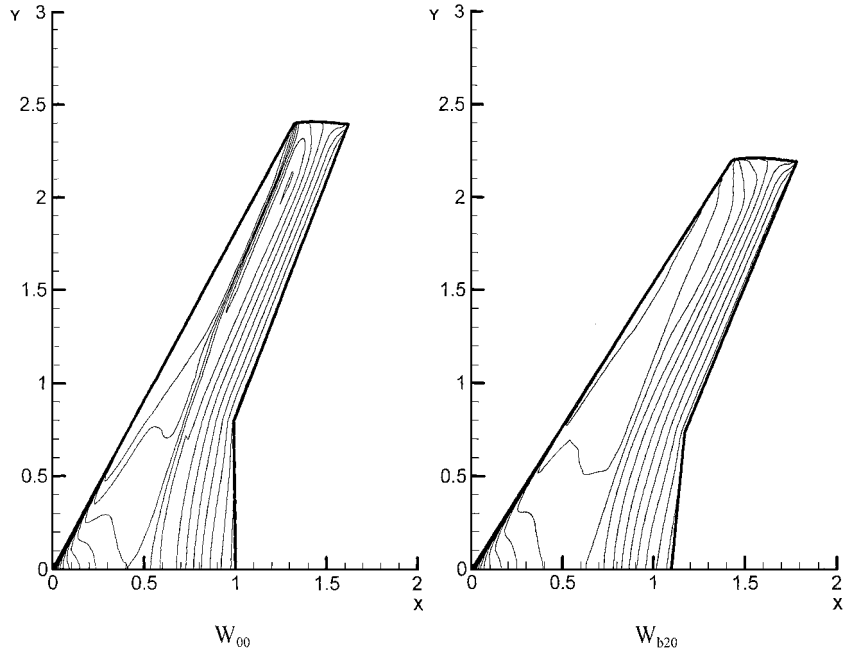

Fig. 6 Pressure contours of W_{00} and W_{b20}

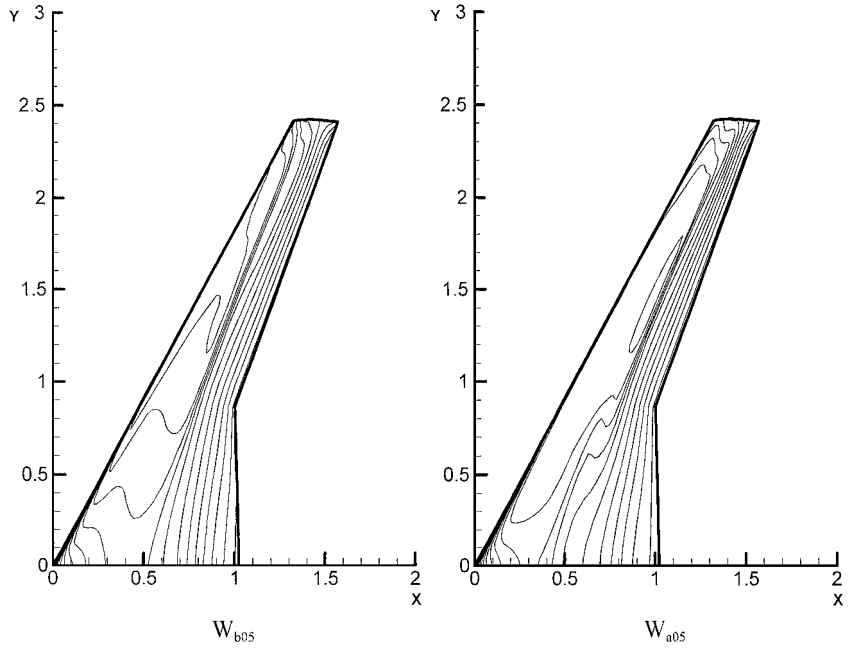

Fig. 7 Pressure contours before and after inverse design.

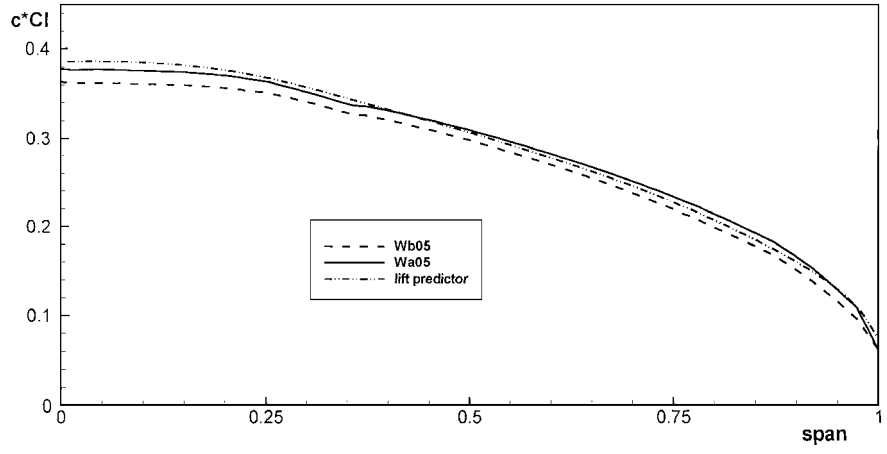

Fig. 8 Spanwise lift distributions at $k = 0.5$.

However, this model was found to give unsatisfactory results. This implies that the variation of wing section lift distributions can not be approximated with enough accuracy by a quadratic RSM whereas the discrepancy between the results of the CFD and Weissinger's lifting line theory can be modeled well by the quadratic RSM.

Estimation of Drag and Weight

The wing drag and weight should also be estimated to find an optimum wing that has the minimum drag and weight. Although the drag data of the 65 wings analyzed for the response surface construction are known, they can not be used for the estimation of drag of candidate wings because section shape parameters are not included in the design variables for the response surfaces.

We estimated an induced drag from a spanwise lift distribution obtained by the lift prediction model. The profile drag coefficient of wing section is calculated by a quadratic function method.[19] To estimate the magnitude of the wave drag coefficient of a swept wing section, the following relation is used[2]:

$$C_{d_w} \cong 0.04/(t/c)^{1.5}\left[M_s \cos\theta_s - \left(1.1/\cos\Lambda_{\frac{1}{2}}\right) + 0.1\right]^4 \quad (16)$$

where θ_s is a shock sweep angle and M_s is a local Mach number in front of the shock. Total wave and profile drag coefficients can be obtained by integrating the section values along the wing span. The total drag of a wing can be estimated by summing up the three drag components. One may expect that the drag data obtained from the CFD calculations can be used.

To estimate the wing weight we used an analytical–empirical method suggested by Torenbeek.[20] The optimum weight is estimated by an analytic method using the wing box model with an assumption that the elastic axis is located at the center of a wing box and that a lift is imposed on the elastic axis. The effect of torsion on the optimum weight and other parts of the wing weight are estimated with a statistical method.

Genetic Optimization

The objective function and constraints are defined as follows:

$$\text{minimize} \qquad \text{drag/drag}_{00} + k \cdot \text{weight/weight}_{00}$$

$$\text{subject to} \qquad \text{lift} \geq \text{lift of baseline wing}$$

where k is a weighting factor and W_{00} is a baseline wing located at the center of the design space. In addition to the lift constraint, 21 constraints are specified to make target pressure distributions reasonable.[2]

For this optimization problem, as mentioned earlier, the number of design variables is 53 (8 for wing planform and 45 for target pressure distributions at 3 design sections).

As pointed out in Ref. 5, the objective function of the target pressure optimization problem is severely nonlinear, and the gradient of the objective function might be discontinuous. Thus, a robust optimization technique that does not use gradient information of the objective function should be used. In the present optimization problem, the situation would be same or worse because it contains the target pressure optimization in it.

A GA is a search algorithm based on the natural selection and the survival of the fittest. It has become popular recently because of its robustness and capability of finding the global minimum. In this study the GENOCOP code (version 2.1),[21] which adopts a GA based on the real number coding, is applied. In the GENOCOP code reproduction is based on the cumulative probability of survival of each population. The agents that die are replaced by a new population generated by seven genetic operators: reproduction, whole arithmetic crossover, simple arithmetic crossover, uniform mutation, boundary mutation, nonuniform mutation, and whole nonuniform mutation. The frequencies of the seven operators are set equal.

Figure 5 shows a flowchart of WTO by the GA. Populations are randomly created, and wing planform and target pressure distributions are constructed for each population. Wing lift, drag, weight, and section maximum thickness-to-chord ratios are estimated, and a fitness value of each population is calculated based on these values. Then the genetic operators are applied to generate new populations of the next generation. This routine is repeated until the maximum generation number is reached.

Design Examples

WTO Results

We conducted the WTO with three different weighting factors: $k = 0.5, 1.0$, and 2.0. W_{b05} represents a wing optimized with $k = 0.5$, W_{b10} with $k = 1.0$, and W_{b20} with $k = 2.0$. The GA was run with the population number of 500 and the maximum generation number of 2000. Required computational time for wing planform and target pressure optimization with GA is about 150 minutes on a DEC alpha 533-MHz workstation.

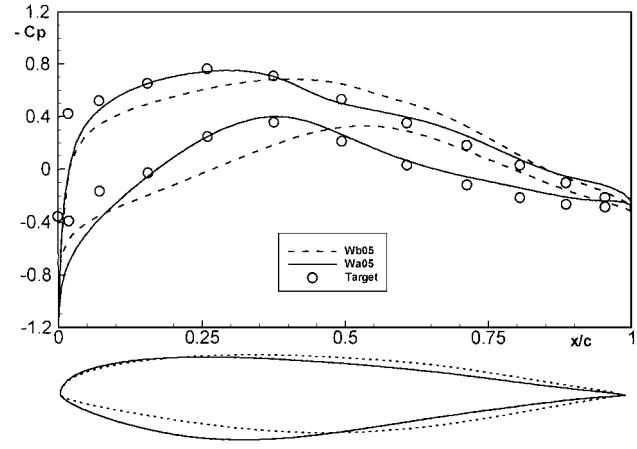

Design section 1

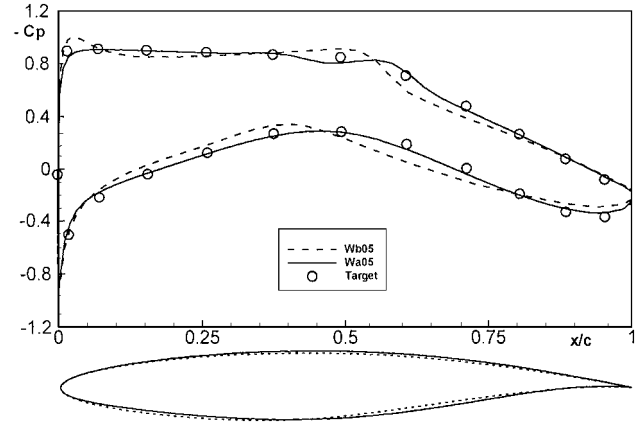

Design section 2

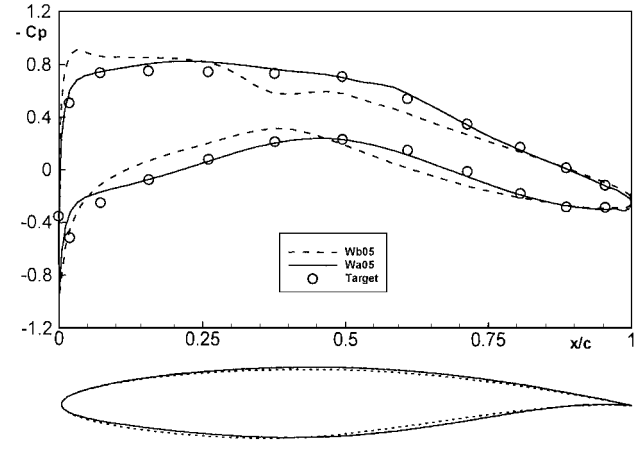

Design section 3

Fig. 9 Pressure distributions and airfoil shapes at $k = 0.5$.

Table 3 shows wing design results by the WTO. Aerodynamic coefficients are obtained by flow analyses. For the flow analysis of the design wings, baseline wing sections are adopted with adjusted maximum thickness. As k increases, $(t/c)_{ds0}$ and C_0 increase, and y_2 and AR decrease to reduce the wing weight. As k decreases, the results show a more improved lift-to-drag ratio (L/D) than those with a larger k. The W_{b05} has the largest lift-to-drag ratio among the design wings and the W_{b20} the smallest weight, whereas the W_{b10} has medium values between those of W_{b05} and W_{b20}.

Figure 6 shows upper surface pressure contours of W_{00} and W_{b20}. The baseline wing W_{00} has a strong shock wave outboard. On the other hand, W_{b20} is shock free because it has a large sweep angle. Thus, we only performed inverse designs for W_{b05} and W_{b10}.

Table 3 WTO results

Parameter	W_{00} (baseline)	W_{b05} $(k=0.5)$	W_{b10} $(k=1.0)$	W_{b20} $(k=2.0)$
Λdeg	29	29.05	27.94	33.16
θ_0,deg	5	4.57	5.26	4.61
θ_2,deg	1	0.65	0.14	0.45
TR_1	0.55	0.51	0.50	0.63
TR_2	0.3	0.24	0.23	0.32
y_1, m	5.36	5.80	5.71	4.98
y_2, m	16.08	16.13	15.24	14.73
C_0, m	6.7	6.85	7.13	7.36
S, m^2	116.7	113.87	110.79	128.03
AR	8.86	9.14	8.38	6.78
C_D	0.02707	0.02482	0.02680	0.02462
C_L	0.5508	0.5223	0.5425	0.4720
L/D	20.37	21.04	20.24	19.17
$(t/c)_{d0}$	0.14	0.133	0.144	0.15
$(t/c)_{d1}$	0.10	0.1149	0.1082	0.117
$(t/c)_{d2}$	0.10	0.115	0.1082	0.117
Weight, kg	6123	5673	5277	5267

Inverse Design Results

Figure 7 compares upper surface pressure contours of W_{b05} and W_{a05}. Shock strength is reduced through the inverse design except at the middle of outboard. However, if we had design sections at the region, we could obtain a shock-free wing. Figure 8 shows lift

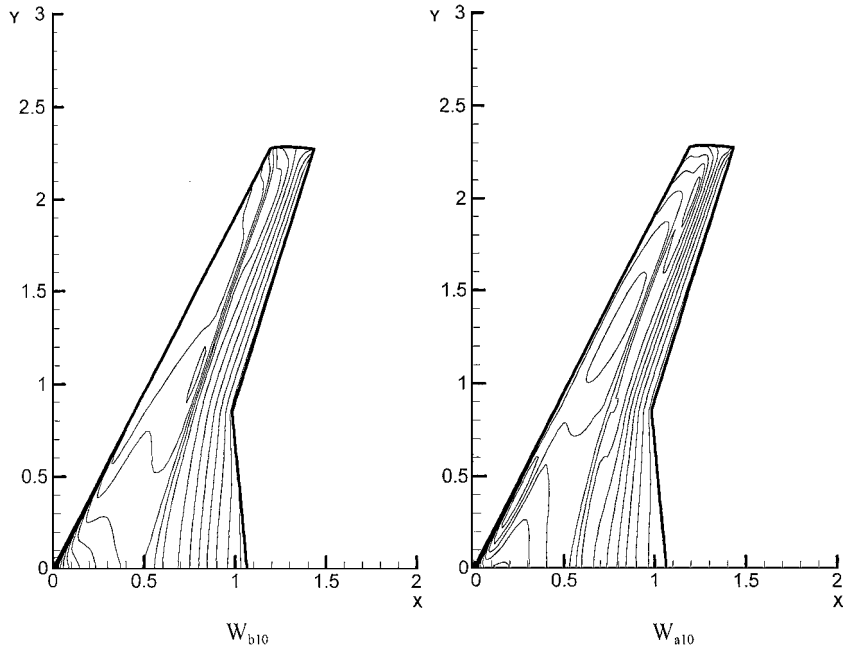

Fig. 10 Pressure contours before and after inverse design.

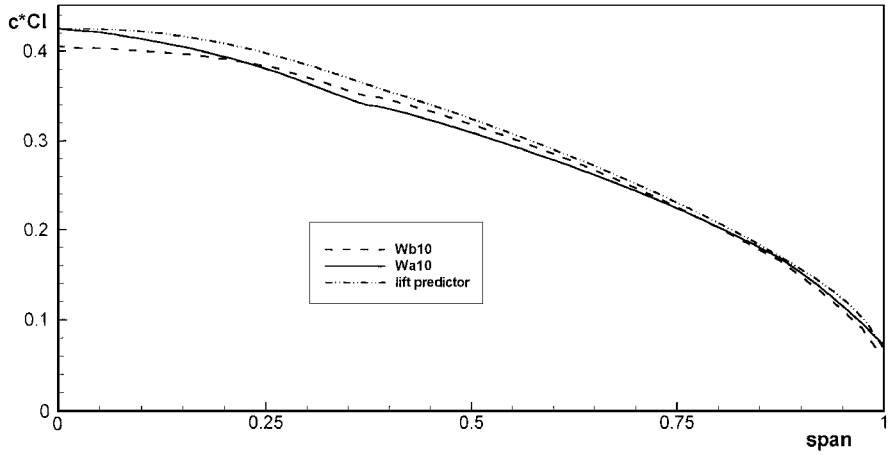

Fig. 11 Spanwise lift distribution at k = 1.0.

Table 4 Inverse design results

Parameter	$k = 0.5$			$k = 1.0$		
	W_{b05}	W_{a05}	Δ, %	W_{b10}	W_{a10}	Δ, %
C_D	0.02482	0.02589	+4.31	0.02680	0.02661	−0.71
C_L	0.5223	0.5471	+4.75	0.5425	0.5432	+0.13
L/D	21.04	21.13	+0.43	20.24	20.42	+0.89
Weight, kg	5673	5703	+0.52	5277	5239	−0.71
$(t/c)_{ds0}$	0.1328	0.1423	+7.2	0.1437	0.1425	−0.8
$(t/c)_{ds1}$	0.1149	0.1177	+2.4	0.1082	0.1054	−2.6
$(t/c)_{ds2}$	0.1150	0.1164	+1.2	0.1082	0.1127	+4.2

distributions of design wings. The W_{b05} result shows a slight discrepancy, whereas the W_{a05} result compares well with that obtained by the lift predictor.

Figure 9 shows target and computed pressure distributions and the wing section geometries of W_{b05} and W_{a05}. Some discrepancy between the target and design pressure at the leading-edge lower surface of the root section is observed. This is because design sections are smoothed and fitted to a 10th-order polynomial in the inverse design code. Except in that region, the target and design pressure distribution coincide extremely well with each other.

Table 4 presents design results before and after the inverse design. For $k = 0.5$, lift and drag coefficients, L/D, and weight are all slightly increased. Thickness-to-chord ratios do not change much except the root design section, which have the lowest adj-R^2 value among the design sections.

Figure 10 compares upper surface pressure contours of W_{b10} and W_{a10}. Note that the outboard shock strength of W_{a10} is remarkably reduced through the inverse design procedure. Figure 11 shows spanwise lift distributions. The lift distribution of W_{b10} shows a slight discrepancy at root section, but that of W_{a10} coincides well with that by the lift predictor. In Fig. 12, target, computed pressure distributions and wing section geometries of W_{b10} and W_{a10} are presented. The pressure distribution of W_{a10} almost exactly coincides with the target pressure distribution. The shock strength at the design section 2 is reduced by the inverse design.

In Table 4 we can see that, when $k = 1.0$, drag coefficient and weight decreased and L/D increased through the inverse design. Thickness-to-chord ratios do not change much through the inverse design, which implies that the RSM for maximum thickness gives accurate prediction results.

In both of the inverse design cases with $k = 0.5$ and 1.0, improvement of aerodynamic performance is not so drastic because the section airfoil used for the baseline wings is known to have good performances at similar design conditions.

Computational Cost

The present approach of WTO can be interpreted as a wing design optimization in which wing section shape parameters are replaced by target pressure distributions. Because of this, the number of design variables for the response surface construction could be greatly reduced so that the computational costs decrease by an order of magnitude. The computational cost of the present design method is mainly due to the 65 flow analyses for the RSM of maximum thickness. Additional costs are caused by 150 min for the genetic optimization of the WTO procedure and by 12 inverse design iteration, which is equivalent to 1.5 times the cost of a flow analysis. Therefore, the total computational cost is not larger than that of 70 flow analyses.

On the contrary, conventional methods using RSM to approximate the aerodynamic coefficients such as C_L and C_D require much higher computational cost. For example, if 3 design sections are employed with 10 geometric shape functions per a design section, the total number of design variables is 38 $(=8 + 3 \times 10)$, and the number of regression coefficients is 780 $[=(38 + 1)(38 + 2)/2]$. This requires more than 1170 flow analyses, which is more than 16 times the cost required by the present approach. This increases rapidly as the number of design variable increases, which is often the case for supercritical wing section design problems.

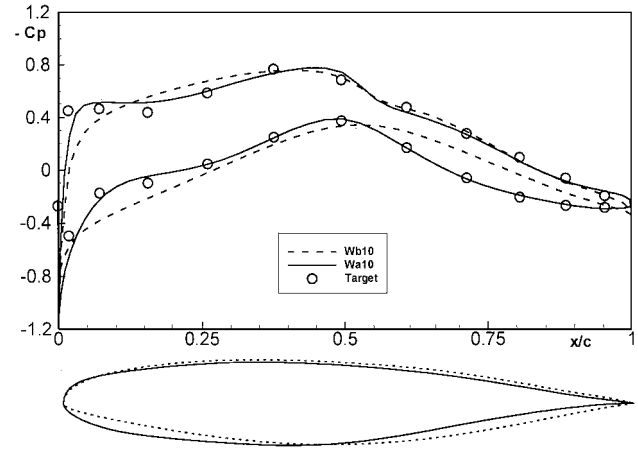

Design section 1

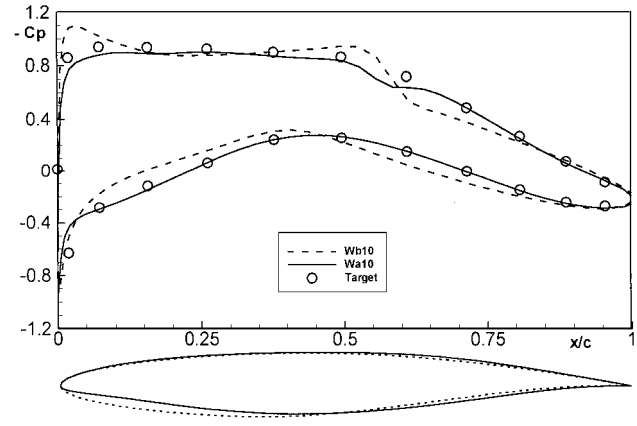

Design section 2

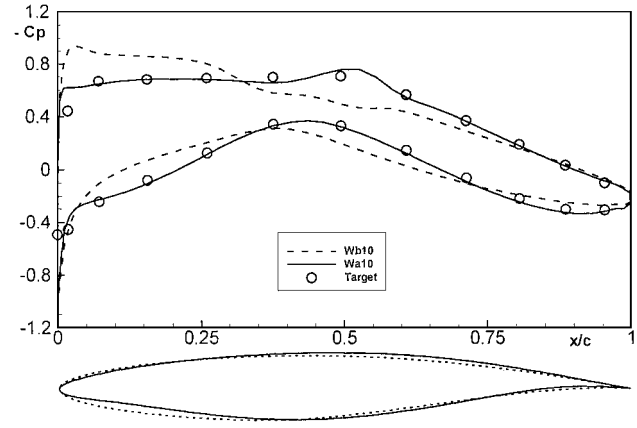

Design section 3

Fig. 12 Pressure distributions and airfoil shapes at $k = 1.0$.

Conclusions

To apply the inverse design method to a preliminary multidisciplinary design problem of finding a transonic wing shape with minimum drag and weight, a target pressure optimization code is extended to optimize wing planform and target pressures simultaneously. During the optimization process, the maximum thickness of wing sections and spanwise lift distributions are predicted by response surfaces. We conducted genetic optimization of wing planform and target pressure distribution for three weighting factors in the objective function. Inverse designs are performed to determine wing section shapes producing the optimized target pressure distributions. Design results show that the present design method gives reasonable wing configurations and requires less than $\frac{1}{16}$th of the computational cost required by conventional direct design approaches with the RSM.

References

[1]Kim, H. J., and Rho, O. H., "Dual-Point Design of Transonic Airfoils Using the Hybrid Inverse Optimization Method," *Journal of Aircraft*, Vol. 34, No. 5, 1997, pp. 612–618.

[2]Kim, H. J., and Rho, O. H., "Aerodynamic Design of Transonic Wings Using the Target Pressure Optimization Approach," *Journal of Aircraft*, Vol. 35, No. 5, 1998, pp. 671–677.

[3]Hager, J. O., Eyi, S., and Lee, K. D., "Two-Point Transonic Airfoil Design Using Optimization for Improved Off-Design Performance," *Journal of Aircraft*, Vol. 31, No. 5, 1994, pp. 1143–1147.

[4]Reuther, J. J., Jameson, A., Alonso, J. J., Rimlinger, M. J., and Saunders, D., "Constrained Multipoint Aerodynamic Shape Optimization Using an Adjoint Formulation and Parallel Computers, Part 1," *Journal of Aircraft*, Vol. 36, No. 1, 1999, pp. 51–60.

[5]van Egmond, J. A., "Numerical Optimization of Target Pressure Distributions for Subsonic and Transonic Airfoils Design," *Computational Methods for Aerodynamic Design (Inverse) and Optimization*, AGARD 463, March 1990.

[6]Obayashi, S., and Takanashi, S., "Genetic Optimization of Target Pressure Distributins for Inverse Design Methods," *AIAA Journal*, Vol. 34, No. 5, 1996, pp. 881–886.

[7]Takahashi, S., Obayashi, S., and Nakahashi, K., "Inverse Optimization of Transonic Wing Shape for Mid-Size Regional Aircraft," AIAA Paper 98-0601, Jan. 1998.

[8]Hwang, S. W., "Numerical Analysis of Unsteady Supersonic Flow over Double Cavity," Ph.D. Dissertation, Dept. of Aerospace Engineering, Seoul National Univ., Seoul, Republic of Korea, Feb. 1996.

[9]van Leer, B.,"Towards the Ultimate Conservative Difference Scheme, V. A Second Order Sequel to Godunov's Method," *Journal of Computational Physics*, Vol. 23, 1979, p. 101.

[10]Jameson, A., and Yoon, S., "Lower–Upper Implicit Schemes with Multiple Grids for the Euler Equations," *AIAA Journal*, Vol. 25, No. 7, 1987, pp. 929–935.

[11]Malone, J. B., Narramore, J. C., and Sankar, L. N., "Airfoil Design Method Using the Navier–Stokes Equations," *Journal of the Aircraft*, Vol. 28, No. 3, 1991, pp. 216–224.

[12]Campbell, R. L., and Smith, L. A., "A Hybrid Algorithm for Transonic Airfoil and Wing Design," AIAA Paper 87-2552, June 1987.

[13]*Jane's All the World's Aircraft*, McGraw–Hill, New York, 1973, pp. 375, 376.

[14]Venter, G., Haftka, R. T., and Stanes, J. H., Jr., "Construction of Response Surfaces for Design Optimization Applications," 6th AIAA/NSSA/USAH/ISSMO Symposium on Multidisciplinary Analysis and Optimization, Belleune, WA, AIAA Paper 96-4040-CP, Oct. 1996, pp. 548–564.

[15]Montgomery, D. C., and Myers, R. H., *Response Surface Methodology: Process and Product Optimization Using Designed Experiments*, Wiley, New York, 1995, Chap. 2, 3, pp. 16–133.

[16]Giunta, A. A., Balabanov, V., Haim, D., Grossman, B., Mason, W. H., Watson, L. T., and Haftka, R. T., "Multidiscplinary Optimization of a Supersonic Transport Using Design of Experiments Theory and Response Surface Modeling," *Aeronautical Journal*, Vol. 101, No. 1008, 1997, pp. 347–356.

[17]Box, M. J., and Draper, N. R., "On Minimum-Point Second-Order Designs," *Technometrics*, Vol. 16, No. 4, Nov. 1974, pp. 613–616.

[18]Gray, W. L., and Schenk, K. M., "A Method for Calculating the Subsonic Steady-State Loading on an Airplane with a Wing of Arbitrary Planform and Stiffness," NACA TN 3030, Dec. 1953.

[19]Wakayama, S., and Kroo, I., "A Method for Lifting Surface Design Using Nonlinear Optimization," AIAA Paper 90-3290, Sept.1990.

[20]Torenbeek, E., "Development and Application of a Comprehensive, Design Sensitive Weight Prediction Method for Wing Structure of Transport Category Aircraft," Rept. LR-693, Delft Univ. of Technology, Delft, The Netherlands, Sept., 1992.

[21]Michalewicz, Z., *Genetic Algorithms + Data Structures = Evolution Programs,* Springer-Verlag, New York, 1992, Chap. 7, pp. 121–154.